Geomorphology 118 (2010) 369–382

Contents lists available at ScienceDirect

Geomorphology

journal homepage: www.elsevier.com/locate/geomorph

# Multi-proxy records of regionally-sourced tsunamis, New Zealand

James Goff [a,*], Steven Pearce [b], Scott L. Nichol [c,1], Catherine Chagué-Goff [a], Mark Horrocks [d], Luke Strotz [a]

[a] Australian Tsunami Research Centre, School of Biological, Earth, and Environmental Sciences, University of New South Wales, Sydney 2052, Australia
[b] Auckland City Council, Private Bag 92516, Wellesley St., Auckland, New Zealand
[c] School of Geography and Environmental Science, The University of Auckland, Private Bag 92019, Auckland, New Zealand
[d] Microfossil Research, 31 Mont Le Grand Rd, Mt Eden, Auckland 1024, New Zealand

ARTICLE INFO

*Article history:*
Received 12 October 2009
Received in revised form 3 February 2010
Accepted 7 February 2010
Available online 13 February 2010

*Keywords:*
Palaeotsunamis
New Zealand
Multi-proxy
Regional sources

ABSTRACT

A multi-proxy study of sediment cores from Kaituna Bay, Mimiwhangata, in northern New Zealand has produced a record of three palaeotsunamis, dated to around 6500 cal yr BP, 2800 cal yr BP, and 1450 AD. These events punctuate a coastal palaeoenvironmental history spanning the last 8000 years or more in which the site progressed from a semi-open lagoon to a freshwater swamp. Proxies used included stratigraphy, geochemistry, palynology, diatoms, foraminifera, geomorphology, and a regional palaeotsunami synthesis. The identification of tsunamigenic sources for these events is tentative. We propose that the two oldest events are associated with a source in the Tonga–Kermadec Trench region, with the most recent possibly associated with the Kuwae caldera collapse in 1452/1453 AD. Palaeotsunami deposits contemporaneous with the estimated age of the three events identified in this study were used to assist in identifying possible source regions. The development of regional and national palaeotsunami databases is in its infancy, but as more data become available, the ability to determine the source, magnitude and frequency of past events will improve. This will greatly enhance our understanding of the regional risk from tsunamis.



## 1. Introduction

Much of the tsunami research carried out since the 2004 Indian Ocean tsunami (2004 IOT) has benefited from detailed interpretations of the deposits related to that event (e.g. Hawkes et al., 2007). Multi-proxy studies of precursor events to the 2004 IOT, however, have tended to focus on a limited range of variables based around standard sedimentary and micropalaeontological options (e.g. Jankaew et al., 2008; Monecke et al., 2008). In the absence of a more extensive suite of proxy data, many of these interpretations hinge upon an understanding of the palaeoenvironmental context of a site at the time of inundation. This is often poorly understood and ultimately leads to what are almost certainly palaeotsunami deposits being termed "probable" as opposed to a more definitive interpretation (e.g. Jankaew et al., 2008; Monecke et al., 2008).

Notwithstanding the input from studies related to the 2004 IOT, significant contributions have been made by researchers to the diversity of usable proxies over the past few years. Until recently, pollen data were generally used to identify a possible marine inundation by using low concentrations of spores to infer a seaward origin (e.g. Goff et al., 2001). Pollen data are now being used more rigorously to indicate the ecological impact of marine inundation as a guide to the environmental significance of an event (Hughes and Mathewes, 2003; Smith, et al., 2004; Dahanayake and Kulasena, 2008; Mamo et al., 2009 and references therein). Geochemical indicators in sediments have tended to be a somewhat forgotten or under-appreciated proxy, and yet are equally as useful as their micropalaeontological counterparts (Chagué-Goff and Goff, 1999; Chagué-Goff, 2010). Like micropalaeontological evidence, the signal varies from site to site and requires appropriate expertise to interpret the data. Archaeological (Bedford, 2006; McFadgen and Goff, 2007), anthropological (King et al., 2007; Terrell et al., in press), and geomorphological (Goff et al., 2008a; Witter, 2008) proxies continue to be recognised and enhanced, and yet are rarely used.

It is through the use of many, as opposed to few, proxies that progress will be made in identifying sediments laid down by palaeotsunamis. It is also becoming more apparent that it is the attention to detail that helps to determine the difference between storms and tsunamis (e.g. Kortekaas and Dawson, 2007). In the case of the 1755 AD Lisbon tsunami and a more recent known storm event, it was minor differences in foraminiferal assemblages and the presence of rip-up clasts in the tsunami deposit that were the key differences (Kortekaas and Dawson, 2007). These were both known events and while the differences were subtle, there were indeed differences. It therefore seems appropriate to anticipate that similar subtle differences between palaeotsunamis and palaeostorms will be found elsewhere, perhaps more so given that the older the deposit the more likely it is to have experienced a loss of integrity due to taphonomic processes (Goff et al., 2007; Hawkes et al., 2007).

* Corresponding author. Tel.: +612 9385 8431; fax: +612 9385 1558.
*E-mail addresses:* j.goff@unsw.edu.au (J. Goff), stevepearce@maxnet.co.nz (S. Pearce), slnichol@tpg.com.au (S.L. Nichol), info@microfossilresearch.com (M. Horrocks).
[1] Current address: Geoscience Australia, GPO Box 378, Canberra ACT 2601, Australia.

0169-555X/$ – see front matter © 2010 Elsevier B.V. All rights reserved.
doi:10.1016/j.geomorph.2010.02.005

In New Zealand, we have the opportunity to use multi-proxy data on largely undisturbed and unstudied coastal sediment sequences formed in a seismically active setting. Like elsewhere in the World, earlier palaeotsunami studies in New Zealand focussed mainly on a limited number of proxies at any one site (the age, stratigraphical position and microfossil content — Goff et al., 2000; age and sedimentology — Nichol et al., 2003a; stratigraphical position and geochemistry — Goff and Chagué-Goff, 1999), while more recently there has been a move towards the use of a larger suite of proxy data (e.g. McFadgen and Goff, 2007).

New Zealand sits astride the boundary between the Australian and Pacific Plates. In historic times seismic activity has ranged from small earthquakes and tsunamis that have caused no damage, to much larger-scale events (de Lange and Healy, 1986; Grapes, 2000). Recent reviews of past tsunamis in New Zealand show that large events, some with a nationwide impact throughout the North and South Islands, have occurred several times in the mid- to late Holocene (Goff and McFadgen, 2002; Goff, 2008; Goff et al., in press). The most recent events occurred around the mid to late 15th Century AD and were linked with a cluster of large earthquakes and associated tectonic activity (Goff and McFadgen, 2002). Most of this activity took place in the South Island and lower half of the North Island, but the highest elevation palaeotsunami deposits around this time are found in the northern North Island (Nichol et al., 2003a, 2003b). The age and source of this particular tsunami have remained elusive with tentative suggestions including subduction along the Tonga–Kermadec Trench and caldera collapse of the submarine Healy volcano with an age possibly within the last 1000 years (Nichol et al., 2003a). Earlier possible palaeotsunamis have also been noted in the sedimentary record of the northern North Island at Rangihoua Bay (Horrocks et al., 2007) and Harataonga Bay, Great Barrier Island (Nichol et al., 2007a). The New Zealand palaeotsunami database is now sufficiently large to allow new palaeotsunami studies to be placed in the wider geographical context of a number of contemporaneously aged events. The opportunity therefore exists to apply similar techniques to those of Smith et al. (2004) where numerous multi-proxy records were used to examine the geographical extent of the Storegga Slide palaeotsunami in the UK. Significantly, as with many countries worldwide, sources for most palaeotsunamis in New Zealand are unknown. The geographical spread of contemporaneously aged events, however, can be used to indicate likely palaeotsunamis source areas (Goff et al., in press).

In this paper we present an account of coastal flooding recorded in contiguous back barrier wetlands in NNE North Island, New Zealand. No historically documented accounts of high-energy events are reported for the area and we therefore have had to rely solely upon the extensive use of proxy data to aid interpretation.

## 2. Kaituna Bay, Mimiwhangata

Kaituna Bay is located on the NNE coast of the North Island at the north end of a small peninsula enclosing Mimiwhangata Bay (35°25′50″ S, 174°25′47″E) (Fig. 1). Local geology is greywacke, varying from soft heavily weathered 'brown rock' to hard jointed siltstones and massive sandstones (Ballantine et al., 1973). Sedimentary environments within Kaituna Bay include a beach and dune barrier system between greywacke outcrops enclosing two freshwater wetlands. The dune barrier system is approximately 350 m long, extends inland up to 80 m from high water, and ranges in height from 4 to 7 m. The smaller (northern) wetland occupies a fully enclosed basin with a catchment area less than 2 $km^2$ and slopes that rise to 20 masl. The wetland has ephemeral standing water and is vegetated by common wetland species dominated by *Typha* spp. The larger (southern) wetland has a catchment area of ~12 $km^2$ with slopes rising to 60 masl. It has a permanent standing water body fringed by *Typha* spp. A low density scatter of sub-rounded greywacke marine pebbles is found on the drainage divide between the two wetlands.

The bay is sheltered to the east and northeast by several islands and rocky islets. Waves approaching from these directions are refracted and diffracted in water depths less than 10 m, to the extent that the beach at Kaituna Bay experiences maximum wave heights of less than 4 m (Gorman et al., 2003). Average tidal range is around 1.5–2.0 m. Beach and dune sediments are medium-coarse sand with minor gravel content. Offshore sediments, however, are dominated by coarse gravelly sands and cobble sized clasts.

## 3. Data sources and analytical techniques

Two continuous sediment cores were extracted from the wetlands by vibrocorer. Core sites were surveyed in to high tide. Core M1 was taken from the seaward side of the smaller wetland to a depth of 4.85 m and core M2, from the seaward side of the larger wetland, reached a depth of 4.1 m (Fig. 1). Core lengths have been adjusted for compaction. In the laboratory, cores were split lengthwise, logged, and sampled for grain size, loss on ignition, geochemistry, foraminiferal, diatom, and pollen analyses, and radiocarbon dating. Grain size analysis followed the procedure of American Society for Testing and Materials (ASTM) (1995). Loss on ignition (LOI) and geochemical analyses adopted the techniques described by Chagué-Goff et al. (2000). Diatom sample preparation followed Devoy (1983). Diatom identification was based on standard diatom floras (Foged, 1979; Krammer and Lange-Bertalot, 1997a, 1997b, 1997c, 1997d; Van der Werff and Huls, 1960, 1961, 1962). Species were grouped according to salinity preference. Samples collected for pollen analysis were prepared using the method of Moore et al. (1991). Podocarp pollen is typically difficult to identify and as such only *Dacrydium* is specified while all other podocarps are listed under the 'undif. podocarps' pollen type. For foraminiferal analysis, samples were washed through a 63 μm sieve to remove the mud sized fraction and allowed to dry in an oven set at low temperature (30 °C or less). To isolate foraminifera tests in the residues, samples were floated using sodium polytungstate separation. Foraminifera were then picked, identified and counted using a binocular microscope. For chronological control, four samples of organic material were taken from core M1 and one from core M2 and submitted to the University of Waikato Radiocarbon Dating Laboratory (Table 1).

## 4. Results and interpretation

### 4.1. Stratigraphy and LOI (M1, M2) Figs. 2–4

Both cores yielded a similar stratigraphy (Fig. 2). The lower facies in each core comprises compact and weathered mud that is massive to faintly laminated, with isolated shell fragments. In core M2, shell material includes crushed valves of the shallow marine species *Austrovenus stutchburyii* at 325 cm depth. Organic content is generally low through the mud but is locally higher where rafted wood fragments occur. A bed of medium to coarse sand is preserved within the basal mud of both cores. This sand bed is 17 cm thick in core M1 (385–402 cm depth) and 4 cm in core M2 (248–252 cm depth) and has sharp basal contacts in both cores (Fig. 2). In core M1 the sand bed is normally graded and in both cores the deposit contains mud rip-up clasts from the underlying sediments. Organic content increases markedly toward the top of the sand bed, reflecting the concentration of fine organic debris (Figs. 3 and 4).

A second bed of medium to coarse, moderately sorted sand is preserved at 205–228 cm in core M1 and 124–150 cm in core M2 (Fig. 2). The deposit is also in sharp contact with the enclosing mud, is normally graded and incorporates organic debris that is in higher concentration toward the top of the bed. In both cases, the coarse-grained texture and sharp basal contact with underlying sediment are interpreted as evidence for barrier overwash and transport of beach and dune sand into the wetland. The presence of mud rip-up clasts and organic debris indicate that the flow was high energy but waned to produce normal grading and allow organics to settle out of suspension.

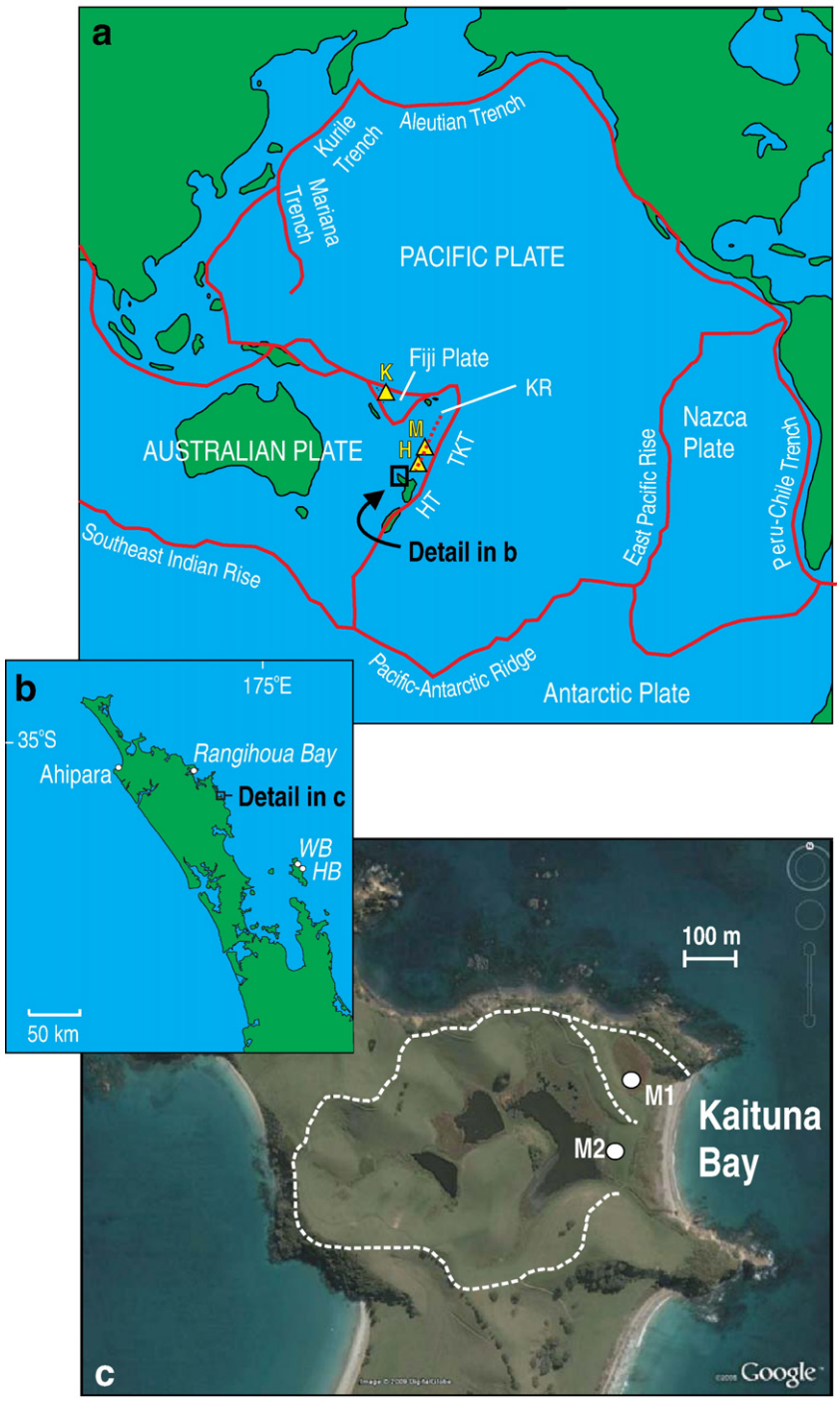


**Fig. 1.** a) New Zealand's tectonic location in the South Pacific with major plate boundaries (H = Healy volcano, K = Kuwae volcano, KR = Kermadec Ridge, M = Macauley volcano, TKT = Tonga–Kermadec Trench). b) Northern North Island, New Zealand showing place names mentioned in the text (WB = Whangapoua Bay, HB = Harataonga Bay). c) Detail of Kaituna Bay, Mimiwhangata showing the core sites M1 and M2 (dashed lines mark the wetland catchment boundaries).

A third, much thicker, coarse-grained deposit forms the uppermost facies of both wetland cores. In core M1 the deposit is 2 m thick and comprises coarse to very coarse sand that is moderately sorted and massive but with local concentrations of gravel to pebble sized clasts of greywacke (e.g. 100, 115, and 150 cm depth). The largest clasts are well-rounded between 8 mm and 16 mm in diameter. Between 60 and 80 cm depth the mud content of the gravel increases to about 15%. In core M2, the equivalent bed is 1.24 m thick and incorporates one well defined layer of gravel clasts at 75 cm depth separating coarse sand above and below. In both cores, organic content is relatively uniform through the sand bed, rising toward the modern surface in the zone of active root growth. Overall, this coarse-grained unit clearly represents another high-energy depositional event (or events), that given the sediment texture can only be associated with barrier overwash.

### 4.2. Radiocarbon ages

Radiocarbon age results for five samples taken from cores M1 and M2 are presented in Table 1 and shown in Fig. 2. Ages show succession up-core from 7930–7680 cal yr BP at 394 cm depth to 2860–2740 cal yr BP at 124 cm depth in core M2. We consider all ages as reliable estimates for enclosing sediments, despite the possibility of

**Table 1**
Radiocarbon data for Kaituna Bay, Mimiwhangata.

| Laboratory number[a] | Core | Depth (m) | CRA[b] ($^{14}$C yr BP) | dC13 (ppm) | 95% CAR[c] (cal. yr BP) | Material dated | Context |
|---|---|---|---|---|---|---|---|
| Wk19431 | M2 | 1.24 | 2719 ± 32 | −27.4 ± 0.2 | 2860–2740 | Organic rich mud | Underlies coarse sand unit |
| Wk19432 | M2 | 2.14 | 5326 ± 42 | −23.0 ± 0.2 | 6190–5930 | Organic rich mud | Within sand unit |
| Wk19433 | M2 | 3.23 | 6570 ± 36 | 1.0 ± 0.2 | 7240–6940 | Cockle (*Austrovenus stutchburyi*) (~5 g dried) | Below sand unit |
| Wk19434 | M2 | 3.94 | 7027 ± 41 | −25.0 ± 0.2 | 7930–7680 | Small wood fragments (~0.2 g dried) | Near base of core |
| Wk19435 | M1 | 3.23 | 5573 ± 47 | −25.0 ± 0.2 | 6410–6200 | Twig (~15 g dried) | Between two sand layers |

[a] Wk = University of Waikato radiocarbon laboratory (the sample from Core M1 was dated using the standard radiometric method, samples from Core M2 were dated using the accelerator mass spectrometer (AMS) method).
[b] Conventional Radiocarbon Age calculated as per Stuiver and Polach (1977).
[c] Calibrated Age Range — all ages have been calibrated using OxCal v.3.10 and southern hemispheric data from McCormac et al. (2004).

reworking of some material (e.g. wood) as this can only have been locally sourced and therefore carries an acceptable in built age (if any) (McFadgen, 2007). The oldest calibrated age indicates that sediments at the base of core M2 (and core M1 by stratigraphic correlation) were probably laid down when sea level was a few metres below present (Gibb, 1986). These dates provide maximum age limits for overlying sediments. The single age obtained from core M1 of 6410–6200 cal yr BP at 323 cm depth is broadly consistent with the age of sediments in core M2 at 214 cm depth.

### 4.3. Geochemistry (core M1 — Fig. 3)

Sulphur (S) concentrations are highest in the sediments below 416 cm (1.85%), lower in the overlying sands, and generally decrease with decreasing depth in the mud-rich layer (between 248 and 378 cm). There are however, several peaks in S up-core. A minor peak occurs between 385 and 402 cm in the sand bed, a spike in concentration between 214 and 228 cm within the sand-dominated unit, and three small peaks at 94, 55 and 20 cm depth (Fig. 3). Chlorine (Cl) concentrations are generally low in most samples, with a gradual increase from 67 cm up-core to the surface. A small peak in Cl concentration between 214 and 228 cm depth, however, coincides with a larger spike of S. The highest Cl concentration occurs in the uppermost sample at approximately 20 cm depth.

Sodium (Na) and strontium (Sr) distributions appear to be closely linked, both showing a general inverse relationship with organic content (LOI). There is almost no correlation between Na/Sr and S, except where peaks in all three elements occur in the sand units at 220–224 and 385–402 cm depth. Iron (Fe) concentrations exhibit marked peaks in the organic-rich unit below 416 cm depth and at

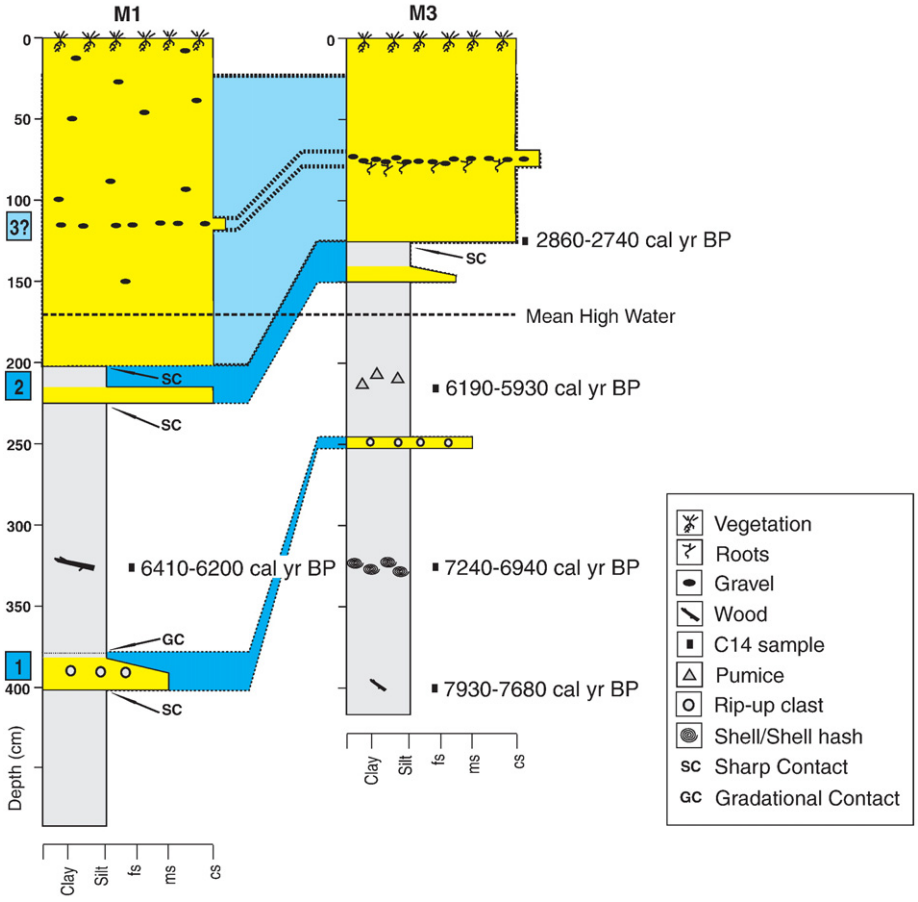


**Fig. 2.** Stratigraphy of cores M1 an M2 showing three stratigraphically correlated events, 1, 2, and 3. The light blue shading is bounded by two different sets of dashed lines for Event 3 — these outline the two possible interpretations discussed in the text. Refer to Table 1 for details of radiocarbon dates (fs = fine sand, ms = medium sand, cs = coarse sand).

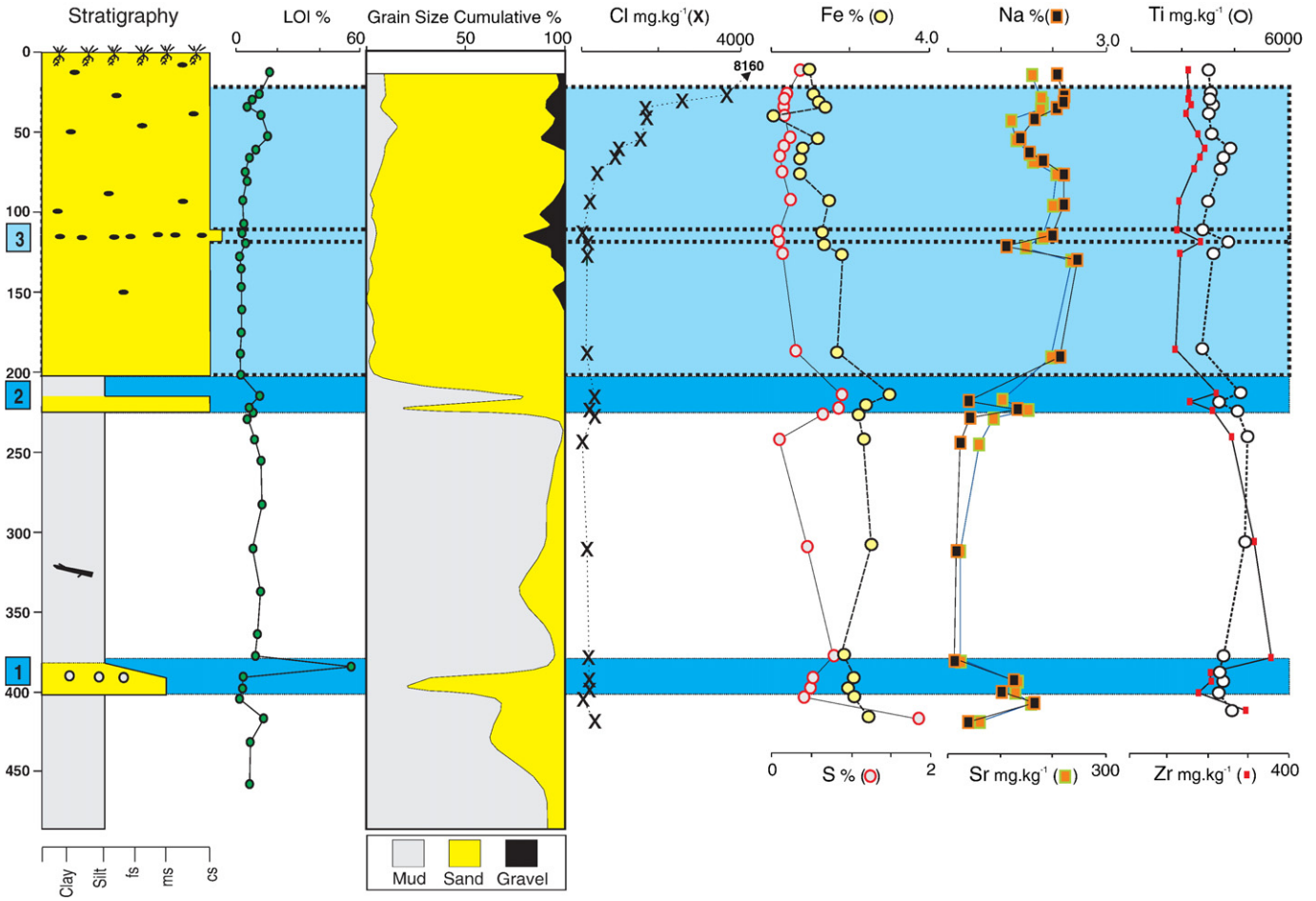


**Fig. 3.** Detail of Core M1 showing stratigraphy, Loss on Ignition (LOI), grain size, and elemental composition (Cl, S, Na, Sr, Ti, and Zr). The light blue shading is bounded by two different sets of dashed lines for Event 3 — these outline the two possible interpretations discussed in the text. Refer to Table 1 for details of radiocarbon dates (fs = fine sand, ms = medium sand, cs = coarse sand).

214–217 cm depth. Fe concentrations however, are lower in the underlying layer (220–228 cm), which is marked by peaks in S, Na and Cl.

Elemental distribution in coastal wetland ecosystems has often been used as a proxy for palaeosalinity, mainly because a number of elements, such as S, Na, Cl, and Sr, occur in higher concentrations in seawater than in freshwater (López-Buendia et al., 1999; Chagué-Goff and Goff, 1999; Chagué-Goff et al., 2000, 2002). While S in brackish peat and clay often occurs in organic form, and results from the uptake of sulphate from seawater (Lowe and Bustin, 1985; Dominik and Stanley, 1993; Chagué-Goff et al., 2000), it can also occur as pyrite in association with iron (Fe), when Fe is present (e.g. Varekamp, 1991; Chagué-Goff and Goff, 1999; Goff and Chagué-Goff, 1999). Cl occurs often in association with Na, but its uptake is strongly related to the organic matter in the wetland sequence (Chagué-Goff and Fyfe, 1996).

In core M1, S peaks occur not only in strong association with the organic matter (below 416 cm, at 376–378 cm and at 214–217 cm depth), but also in sandy layers characterised by low organic content (at 220–228 cm depth). S also appears to be fairly closely linked to iron ($r^2 = 0.61$), and is likely to occur as pyrite in the sediment. Concentrations are typical for brackish clays (Lowe and Bustin, 1985) and thus reflect the influence of seawater in the wetland. Although S concentrations decrease up-core between 378 and 248 cm depth in the muddy layer, there are not enough data to indicate whether the decrease was sudden or progressive. A marine influence in the thin sandy layer overlying organic-rich mud (220–224 cm depth) is corroborated by the presence of Cl, Na and Sr.

In addition to peaks in S, there are marked peaks in the constituent elements of heavy minerals such as zircon (Zr) and titanium (Ti). Both have peaks around 390 cm, 216 cm, 120 cm, and 61 cm depth. The first three peaks coincide with a band of increased elemental concentrations that are associated with higher palaeosalinity. The uppermost peak occurs in a section of core between 0 and 120 cm depth where there are marked fluctuations in all the elements discussed above.

### 4.4. Pollen (core M2 — Figs. 4, 5a, 5b)

Tall trees and shrubs dominate the pollen sum in the mud of the lowermost sample (at 410 cm depth). The conifer component of the conifer–hardwood forest on the hills surrounding the core site in pre-human times (3.94 cm depth: 7930–7680 cal yr BP) comprised mainly *Dacrydium* (rimu), *Libocedrus* and undifferentiated podocarps. *Metrosideros* was the dominant hardwood and *Cyathea* tree ferns were common in the forest sub-canopy. Shrubs are dominated by *Hebe*; having local pollen dispersal this taxon would have been common in the immediate vicinity of the core site. *Laurelia* (pukatea) trees were also present in the immediate area. The latter, also with local pollen dispersal, is characteristic of wet alluvial soils and base-rich swamps, and is commonly found in lowland semi-swamps and gully forests (Allan, 1961; Macphail and McQueen, 1983). The vegetation in the immediate vicinity of the core site was most likely freshwater swamp forest with gaps occupied mainly by *Hebe*, and also *Leptospermum scoparium*.

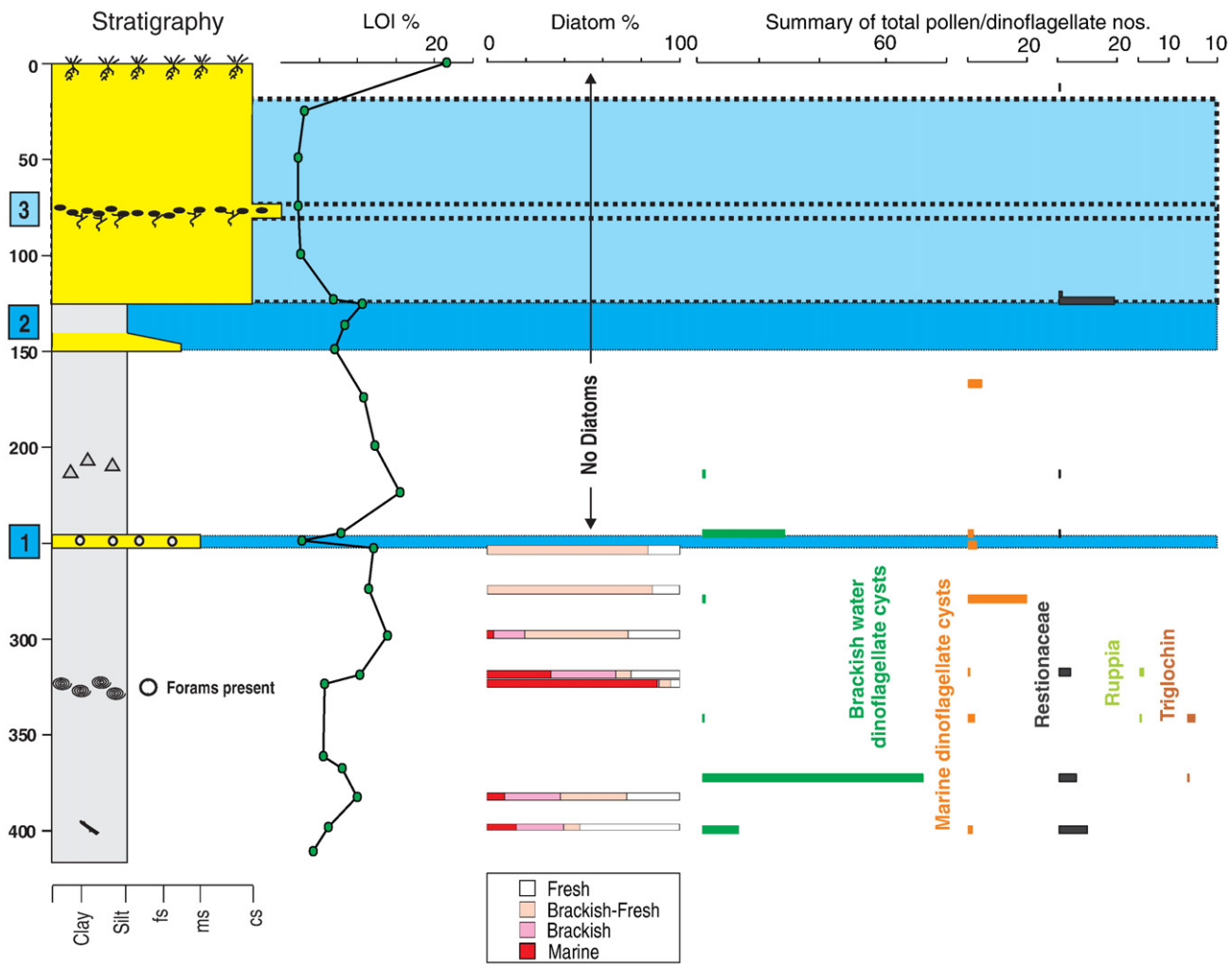


**Fig. 4.** Detail of Core M2 showing stratigraphy, Loss on Ignition, diatom, foraminfera and key pollen data. The light blue shading is bounded by two different sets of dashed lines for Event 3 — these outline the two possible interpretations discussed in the text. Refer to Table 1 for details of radiocarbon dates (fs = fine sand, ms = medium sand, cs = coarse sand).

Above this depth, commencing at 400 cm, *Hebe* declines and brackish-water and marine dinoflagellate cysts appear. The coincident appearance of Restionaceae, *Ruppia* and *Triglochin* also indicate increased salinity. The latter, often sward-forming, is common on the coast in salt marshes (Allan, 1961). The general reduction in local tree and shrub cover was probably due to initial Holocene marine trangression, although *L. scoparium* shrubs increased in the wetland. These more saline conditions continue up-core until 252 cm depth where the presence of the freshwater alga *Botryococcus* suggests a reduction in salinity. This taxon tends to occur in low-energy environments, free from suspended sediment and sub-aerial plants, but surrounded by scrub and in water containing some products of humic degradation to supply nitrogen for growth (Dulhunty, 1944). Pollen of Cyperaceae (sedges) increases markedly at this core depth, indicating a progressive infilling and increasing vegetation cover of the wetland.

Analysis of samples taken from immediately below and above the sand bed at 252–248 cm depth revealed little change in pollen and spore frequencies. However, a distinct increase in brackish-water dinoflagellate cysts suggests a change in salinity associated with the sandy layer, possibly due to barrier overwash (Fig. 5a).

At 125 cm depth, Cyperaceae and Restionaceae show a sharp increase and *Cyathea* shows a marked decline. Also introduced at this point is Malvaceae, most likely *Plagianthus divaricatus* shrubs which are tolerant of saline conditions, reflecting further infilling of the swamp, changing sediment characteristics, and a marine influence. Pollen at the base of the upper sand layer showed a high degree of abrasion most probably indicative of water-transport.

The samples from the upper sand layer (0–124 cm) showed a high degree of pollen corrosion (i.e. degradation by aerobic micro-organisms) and much lower pollen concentrations. The high Malvaceae percentages in the samples from 70 to 52 cm depths (~100%) are probably in part due to differential pollen preservation. Lack of indicators of early Polynesian activity (e.g. *Pteridium*) in the sand samples strongly suggests that this layer was deposited prior to human arrival in the catchment. The sample from 70 cm depth showed a high clay content, indicating disturbance of the surrounding hill slopes.

The uppermost sample of core M2, at 17 cm depth, provides evidence for human impact in the region. There is a paucity of forest pollen types, and pollen indicators of Polynesian (*Pteridium*, Anthocerotae, microscopic charcoal) and subsequent European (*Pinus*) activity are present.

### 4.5. Diatoms (core M2 — Fig. 4)

Fossil diatoms are moderately well preserved between 252 cm and 398 cm depth in core M2. Diatoms are absent or in low abundance above this horizon. In the lowest part of the core (398 cm depth) freshwater (OI — Oligohalobion indifferent) taxa including *Achnathes*

*saxonica krasske*, *Achnanthes hungarica*, and *Navicula placentula* dominate (>51%), but give way to an increasing concentration of brackish-fresh (M — mesohalobous) taxa such as *Cyclotella meneghiana* and *Nitzschia marginulata* at 381 cm depth. In both instances however, two marine taxa (P — polyhalobous) *Cocconeis distans* and *Paralia sulcata*, are present (398 cm: 15.3%; 381 cm: 9.3%). The diatom assemblage at this interval suggests a moderate marine influence. The marine diatoms are sparse and often broken, indicating that they have probably been washed in from nearshore, sandy marine sediments. There is a diatom barren zone between 381 and 323 cm depth, followed by a section of core with good abundances and preservation of diatoms up to 252 cm depth.

At 323 cm depth, marine (Polyhalobous) diatoms, in particular *P. sulcata*, account for nearly 90% of the count. Chronologically, this core depth correlates with the end of post-glacial sea level rise (Gibb, 1986) (Table 1). Furthermore, samples from this depth are about 1.5 m below the present high water mark (Fig. 2). Up-core there is a gradual change from predominantly marine (P) to almost exclusively brackish-fresh (M — *C. meneghiana*, OI — *Pinnularia* sp.) diatom taxa. This is a zone of marked desalinisation and a progressive isolation of a low-energy freshwater environment from direct marine influence. Chronologically, this occurred immediately following the Holocene stillstand around 6500 years BP (Gibb, 1986), at a time when coastal barrier systems were developing (Table 1).

The uppermost sample at 252 cm depth was taken from near the base of a sand layer. This sample has low abundance of identifiable diatoms, with an assemblage similar to the underlying mud dominated by brackish-fresh (M — *C. meneghiana*, OI — *Pinnularia* sp.) diatom taxa. This weak but consistent diatom signal suggests a stable, low-energy freshwater environment in close proximity to the sea. The sandy sample also contains a high proportion of broken frustules, indicating post-mortem transport with the sand, with the most likely source being the nearshore, beach and dune deposits adjacent to the wetland.

### 4.6. Foraminifera (core M2 — Fig. 4)

Only one sample, taken at 330 cm depth, yielded foraminifera, from which 180 well preserved specimens belonging to four taxa are identified. The dominant fauna is *Ammonia aoteana* (Finlay), comprising 97.5% of the assemblage. Three other taxa, *Pileolina zealandica* Vella, *Quinqueloculina seminula* (Linnaeus) and *Quinqueloculina tenagos* (Parker) are present in low abundance (1%, 1% and 0.5%, respectively). All four taxa are common constituents of estuarine and inner shelf foraminiferal faunas throughout New Zealand (Hayward et al., 1999) and the south-west Pacific (Yassini and Jones, 1995; Strotz, 2003). *A. aoteana* is found in a broad suite of ecological conditions, but high relative abundances are largely confined to middle estuary settings, particularly low-energy basin-style settings where organic, nutrient-rich substrates prevail (Yassini and Jones, 1989; Hayward et al., 1999), or to stressed environments around areas where freshwater input occurs (Jorissen, 1988). *P. zealandica* is restricted to open marine conditions, such as the seaward section of estuaries or inner shelf environments (Yassini and Jones, 1995; Strotz, 2003). *Q. seminula* and *Q. tenagos* are both typically confined to fully marine or slightly brackish settings (Hayward et al., 1999). Given the high proportion of *A. aoteana*, the fauna from this sample is taken to be indicative of a semi-open lagoon under marginal marine conditions. The presence of diatoms indicative of marine and marginal marine conditions in other parts of the core suggests the absence of forams from other parts of the core is due to taphonomic (e.g. high acidity) rather than ecological factors.

## 5. Interpretation of environmental changes

Pollen and sediment data indicate that the palaeoenvironment represented at the base of cores M1 and M2 was most likely a lowland semi-swamp or gully forest. This changes markedly with Holocene sea level rise to become a semi-open lagoon system as indicated by brackish-water and marine dinoflagellate cysts and the coincident appearance of Restionaceae, *Ruppia* and *Triglochin* above 400 cm depth, the marginal marine foraminiferal assemblage at 330 cm, the presence of intact bivalves (*A. stutchburyii*) at 325 cm, and a distinct increase in the polyhalobous diatom *P. sulcata* above 323 cm in core M2. The start of barrier formation and the establishment of a low-energy, freshwater wetland is marked by a noticeable increase in organic content above the shell unit at 325 cm (M2). While diatom and pollen data indicate that saline conditions continued to influence the site, a change at 252 cm (M2) represented by the occurrence of the freshwater alga *Botryococcus*, indicates that isolation from the sea was complete by this stage, sometime around 6500 years ago (Fig. 2).

Freshwater conditions have prevailed through to the present day. The uppermost sample from core M2, at 17 cm depth, represents the first clear evidence of human impact at the site. Pollen indicators of both Polynesian (*Pteridium*, Anthocerotae, microscopic charcoal) and European (*Pinus*) activity are present. Low pollen counts in the coarse-grained sediments between 99 and 17 cm depth in core M2 may account for the lack of evidence of human impact further downcore.

This late Holocene palaeoenvironmental framework provides the context for three clear disturbance events at Kaituna Bay, as recorded by the discrete sand-rich deposits in both wetland cores. To varying degrees, these are recognised in the proxy data as marine inundation events (Table 2).

### 5.1. Event 1

This is marked by the deeper sand bed in both cores and bears several significant proxy markers that can be used to infer probable tsunami inundation (Table 2). The unit fines upwards and LOI data indicate that organic material is in higher concentrations in the upper part of the bed. Both are indicators of high-energy flows that gradually wane as opposed to highly variable energy levels more closely associated with storms. Brackish-water and marine dinoflagellate cysts are present in the sand, and the saline-tolerant sedge Restionaceae and Malvaceae shrubs both appear in the pollen record at the top of this unit. Other proxy data are shown in Table 2. Of note is an inwashed, predominantly marine diatom assemblage coupled with a distinct geochemical signature for marine inundation (Na and Sr). Peaks in Ti and Zr may be attributed to an influx of fine detrital mineral matter as a result of primary settling (Blomqvist and Larsson, 1994), but equally it could indicate heavy minerals deposited during a high-energy overwash event (Switzer et al., 2005).

### 5.2. Event 2

In core M1, a fining-upward deposit (from coarse sand to silt: 205–228 cm depth) is bound by upper and lower sharp contacts. This has been stratigraphically correlated with a similar sequence in M2 (124–150 cm depth). The sequence is up to 26 cm thick and contains distinct proxy markers of raised salinity levels (Table 2). LOI data indicate that organic material is in higher concentrations in the upper part of the unit where the pollen record indicates an increase in plants tolerant of saline conditions and indicative of further wetland infilling. The high degree of spore abrasion coupled with a distinct saline geochemical signal (peaks in S, Cl, Na, and Sr) points to marine inundation. Like Event 1 though, the origin of peaks in Ti and Zr in the finer fraction is equivocal. These peaks could have been caused by either an increase in detrital mineral matter as a result of primary settling (Blomqvist and Larsson, 1994), or as heavy minerals deposited during a high-energy overwash event (Switzer et al., 2005).

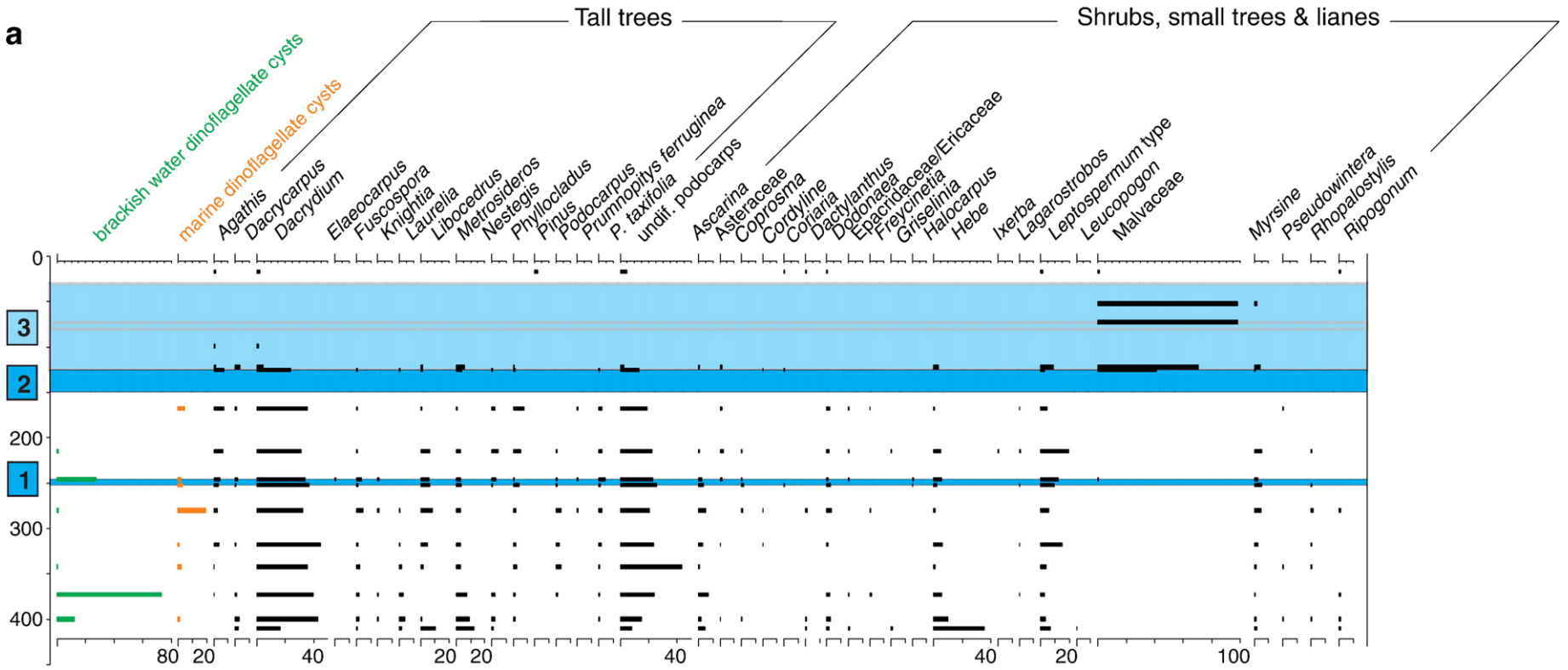


**Fig. 5.** Pollen sum data for core M2: The light blue shading is bounded by two different sets of grey dashed lines for Event 3 — these outline the two possible interpretations discussed in the text. Refer to Table 1 for details of radiocarbon dates (fs = fine sand, ms = medium sand, cs = coarse sand). a) Dinoflagellates, tall trees and shrubs, small trees and lianes; b) Herbs, wetland taxa, and other ferns and allies.

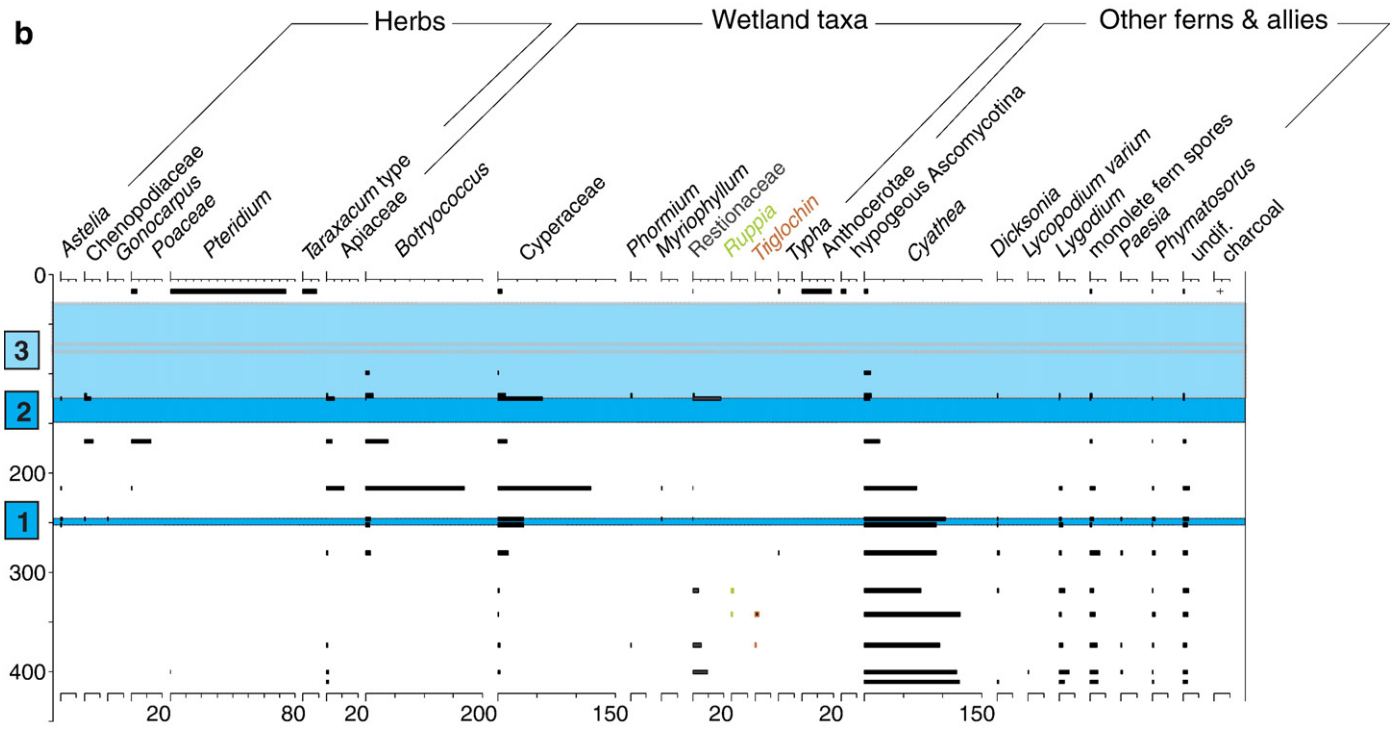


**Fig. 5** (*continued*).

### 5.3. Event 3

The scale of the most recent disturbance event can be interpreted in two ways. First, as a moderate-sized barrier overwash that transported the pebbles and coarse sand preserved at 115 cm depth in core M1 and 75 cm in M2 (Fig. 3). The alternative interpretation is to attribute the full thickness of the uppermost sand and gravel bed found in both cores to one large event. This latter option is supported by strong geochemical indicators of marine inundation throughout the sand, notably S, Na, and Sr. In addition, elevated levels of Ti and Zr indicate a degree of heavy mineral concentration as would result from hydraulic sorting of grains during high-energy transport. Furthermore, in M2 some organic matter appears to be rooted (or contains rooted material?) below the gravel layer and some of this is also incorporated as rip-up within the overlying sediments.

In addition, the elevated levels of Ti and Zr in this coarse sediment layer are interpreted as representing a concentration of heavy minerals (black sand) resulting from hydraulic sorting of grains during high-energy transport. Heavy mineral laminations in tsunami deposits have been widely reported in both recent (2004 IOT) and palaeotsunamis (e.g. Narayana et al., 2007; Nichol et al., 2007b; Morton et al., 2008). Although we did not determine the mineralogy of the sediments in this study, their chemical composition reflects the occurrence of minerals, such as rutile, ilmenite and zircon, which are common constituents of black sand (Narayana et al. 2007).

Are there any other proxy data that can assist in resolving the detail in this particular deposit? In core M1, localised peaks in organic content within the coarse sand record the preservation of rafted organic debris; the first at 116 cm depth comprises fine organics directly beneath the gravel layer and the second between 40 and 60 cm comprises rip-up material. The presence of these separate concentrations of organic debris provides some indication of fluctuations in flow velocity, but is not compelling. In both cores, the uppermost part of the sand bed incorporates slightly more organic material and mud. This may indicate inwash of slope material but equally, in situ production by the modern wetland is also possible. Other proxies (forams, diatoms, and pollen) are poorly preserved to absent within the coarse sand. However, the few pollen grains that are preserved are very corroded which is likely due to degradation by aerobic micro-organisms, and is consistent with initial deposition in beach and dune sands, and subsequent reworking. Overall, the evidence suggests the reworking occurred rapidly, presumably in one event.

Further evidence for this event being the largest in the sediment record is given by the low density scatter of sub-rounded greywacke marine gravels on the drainage divide between the two wetlands, which could indicate widespread inundation. There are no terrestrial sources of marine gravels in the surrounding catchments, but gravels are present in the modern dunes, in the nearshore zone and offshore (Ballantine et al., 1973). This is the most recent deposit identified and it is reasonable to assume that the barrier would have been at or near present day height. With a maximum storm surge of about 1 m, it would require waves of 3 to 6 m high to overtop the present barrier. Given the sheltered aspect of the beach, it is believed unlikely that storm waves would overtop the barrier at Kaituna Bay. Tsunami run-up is therefore the most likely transport mechanism for this deposit.

## 6. Age of events

Three anomalous sand deposits have been identified within the stratigraphy of Kaituna Bay, Mimiwhangata. The earliest, Event 1, is dated to between 6190–5930 cal yr BP and 7240–6940 cal yr BP in M2, and older than 6410–6200 cal yr BP in M1 (Fig. 2, Table 1). The radiocarbon sample in M1 was a twig. This most likely has a small inbuilt age, while the younger date in M2 was obtained from a bulk sample of organic-rich mud which can contain inwashed material (McFadgen, 2007). A bracketed age between 7240–6940 cal yr and 6410–6200 cal yr BP would seem most reasonable, possibly closer to the younger age range.

Event 2 is dated to between 6190–5930 cal yr BP and 2860–2740 cal yr BP in M2, and is younger than 6410–6200 cal yr BP in M1 (Fig. 2, Table 1). The younger organic-rich mud was taken from the top of the fining-upwards sequence in M2. There are two possible scenarios. The organics could be contemporaneous with inundation —

**Table 2**
Proxy data used for Kaituna Bay, Mimiwhangata (after Goff et al., 2001; Dominey-Howes et al., 2006; McFadgen and Goff, 2007).

| Potential proxy evidence of tsunami inundation | Event | | | Comments |
|---|---|---|---|---|
| | 1 | 2 | 3 | |
| Sediments fine inland and/or upwards — relict features such as gravel pavements present. Deposits often rise in altitude (run-up) | √ | √ | √ | Some fining-upwards present |
| Each wave can form a distinct sedimentary sub-unit | | | ? | Events 3 is open to at least two interpretations (see text) |
| Lower contact is unconformable or erosional | √ | √ | √ | |
| Contains intraclasts of reworked material (rip-up) | √ | | √ | |
| Loading structures at basal contact | √ | | | Not observed for Events 2 and 3 |
| Contains increased abundance of marine diatoms and/or reworked terrestrial assemblages | √ | | | No diatoms preserved in sediments for Events 2 and 3 |
| Contains foraminifera and/or other microscopic marine material | | | | No foraminifera observed |
| Pollen concentrations are diluted | | | √ | |
| Geochemistry: increases in concentrations of sodium, sulphur, chlorine, calcium and magnesium (relative) | √ | √ | ? | |
| Individual shells/shell-rich sub-units present | | | | No shell material found |
| Overlies organic-rich muds/soil/vascular plants | √ | √ | √ | |
| Shell, wood, less dense organic material rafted near top of unit | √ | √ | ? | |
| Often associated with reworked archaeological material | | | ? | |
| Ecosystem response to marine inundation | √ | √ | | |
| Replication at more than one site or in off-site deposits | √ | √ | √ | |
| Possible realistic local and/or distant tectonic sources | √ | √ | √ | |

entrained by the event and deposited as rafted material on top of the deposit, or the material was ripped up and incorporated into the sequence. The latter scenario seems less likely since there is no obvious sign of rip-up, although the sample was taken immediately beneath a sharp, erosional contact with the overlying coarse sand. Therefore, there is most likely a hiatus at this point and we do not

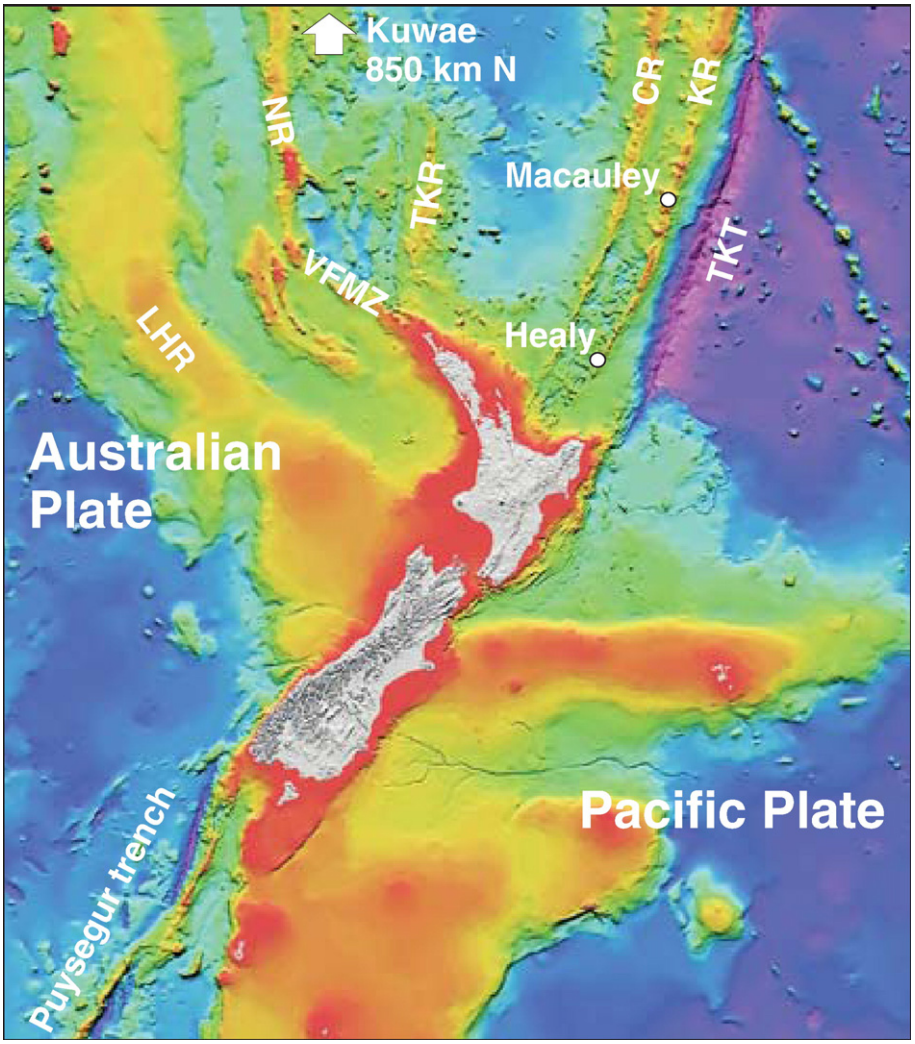


**Fig. 6.** Seafloor bathymetry around New Zealand (modified after CANZ, 1997) indicating features of relevance including the location of two submarine volcanoes mentioned in the text (CR — Colville Ridge, KR — Kermadec Ridge, LHR — Lord Howe Rise, NR — Norfolk Ridge, TKR — Three Kings Ridge, TKT — Tonga–Kermadec Trench, VMFZ — Vening Meinesz Fracture Zone. Bathymetry — shallow, continental shelf (red) to deep trench (purple).

know how much material was eroded. On balance it seems likely that the Calibrated Age Range (CAR) of 2860–2740 cal yr BP may closely approximate the age of the event but with an unknown age between Event 2 and the possible base of Event 3.

Event 3 is dealt with as one deposit since similar arguments apply to the single unit shown in Fig. 2. This deposit is younger than 2860–2740 cal yr BP (M2), but a hiatus of unknown length immediately above the radiocarbon sample means that we do not know how much younger it is. The only evidence for a minimum age is the presence of a coupled Polynesian and European pollen signal at 17 cm depth in M2. Dating of this event is problematic, but it is recognised that one of the most useful proxies for identifying past tsunami inundation is a regionally detectable replication of evidence (McFadgen and Goff, 2007). This particular sequence is unique in the approximately 8000 year record of the bay because it is the only one to contain a high percentage of coarse sand and rounded gravels. Significantly, similar sedimentologically unique deposits have also been reported in northern North Island New Zealand (Nichol et al., 2003a; 2003b; 2004; McFadgen, 2007; Goff, 2008 and references therein). Winnowed, semi-continuous pebble–gravel sheets on exposed coastal dunes up to at least 32 m above present sea level have been dated to around 1480–1500 AD, although the age range could be as much as 1400–1500 AD (McFadgen, 2007). We use the regional extent of this markedly coarse tsunami deposit to infer a similar age for Event 3.

## 7. Regional synthesis

There are few palaeotsunami datasets, but many historic ones. The most comprehensive palaeotsunami datasets include ones for the Cascadia subduction zone in the US Pacific Northwest (Peters et al., 2003), Australia (Dominey-Howes, 2007), New Zealand (Goff, 2008; Goff et al., in press), and Australasia (Goff and Dominey-Howes, 2009). Of these, the Cascadia Tsunami Deposit Database contains data compiled from 52 studies, documenting over 60 sites along the Cascadia margin of western North America. Multiple tsunami deposits found at some sites indicate that as many as 13 tsunamis have affected the coast over the last 7300 years (Peters et al., 2007). This is an extremely comprehensive record for a relatively short length of coast (approx 1300 km) but it clearly shows a common problem for palaeotsunami research — the older the event, the fewer the number of sites. This loss of information with time largely relates to two problems; the taphonomy of a deposit (Horton et al., 2006) and the lack of suitable long-term sedimentary sequences (Goff et al., 2000). For example, it is highly likely that the Kaituna site was inundated by more than these three tsunamis. Some will have been too small to leave any sedimentary evidence at all, and others may have left deposits that have subsequently been lost through exposure to long-term taphonomic processes.

New Zealand does not have the convenience of a single source such as the Cascadia subduction zone (Fig. 6). Source identification from New Zealand palaeotsunami deposits is problematic (Walters et al., 2006). The New Zealand palaeotsunami database has over 330 data points for 30–35 events (Goff, 2008; Goff et al., in press). Like the other datasets, there are a decreasing number of sites for older events, but an attempt at a robust chronological control has been made though a consistent radiocarbon calibration methodology and cross-correlation between sites. There has also been independent validation of events that are reported to have occurred within the last 650 years or so since human occupation (McFadgen, 2007). The variability in the number of possible events is caused by a combination of overlapping age ranges and source interpretations based upon the geographical spread of data points (Goff, 2008; Goff et al., in press). The dataset is small for a coastline of over 17,000 km, but does at least contain sites from all coastal aspects. Linking individual palaeotsunamis with a particular source is difficult. There is relatively limited information about known or potential sources and the possible magnitude of tsunamis they might generate, but with younger events however, there is more information and more valid inferences can be proposed.

Event 1 at Kaituna has been dated to between 7240–6940 cal yr and 6410–6200 cal yr BP, with a possible age of around 6500 cal yr BP or so. There are only four relevant dated palaeotsunami sites within this age range (6200–7240 cal yr BP) and all are at relatively low elevations (used as a proxy for minimum run-up height) (Goff, 2008 and references therein). All are found in the northern North Island of New Zealand (Fig. 7). While this is a small dataset, we would tentatively suggest a source area to the NNE, perhaps related to subduction on the southern part of the Tonga–Kermadec Trench (TKT: Figs. 1a and 6) or towards the northern segment of the Hikurangi Trough (HT: Figs. 1a and 6). Whether a large enough tsunami could be generated to account for the evidence is uncertain (McCann et al., 1979).

Event 2 is considerably younger, with an estimated age of 2860–2740 cal yr BP. There are seven apparently contemporaneous events with a similar, but restricted, regional extent to Event 1 (Goff, 2008 and references therein; Fig. 7). It is not surprising that there are more sites, but it is interesting to note that they cover a shorter length of coastline than those contemporaneous with Event 1. It seems likely therefore, that these sites are associated with a relatively local tsunamigenic source (Fig. 6). Numerical models based upon a comprehensive summary of known faults in the region produced only small wave heights along the affected coast with minimal tsunami inundation (Walters et al., 2006). All known local submarine landslides are either too large, too small, or too old (Lamarche et al., 2008; Walters et al., 2006), and local volcanic sources are similarly too small (Walters et al., 2006). A TKT subduction zone tsunami generated by a smaller earthquake than Event 1 is plausible and fits more reasonably with estimated earthquake magnitudes and tsunami run-up data (McCann et al., 1979; Walters et al., 2006). Alternatively, there are large, regional volcanic sources such as the Healy (H: Figs. 1a and 6) and Macauley (M: Figs. 1a and 6) calderas. Tsunamis could be generated from many southern Kermadec Ridge volcanoes (KR: Figs. 1a and 6) during explosive submarine eruptions (specifically as hot, gas-rich pyroclastic flows) and/or catastrophic sector collapse of the volcanic cone and crater (Lloyd et al., 1996). Eruptive volumes of ~5–100 $km^3$ have been estimated for these volcanoes, with most recent events occurring within the last 10,000 years (Wright et al., 2003, 2006). Walters et al. (2006) point out however, that undersea volcanic sources on the southern Kermadec Ridge can be represented as a point source for tsunamis. Wave amplitudes decrease rapidly with distance from the source and do not produce large tsunamis at the coast. A TKT source therefore seems to be the most plausible scenario.

A brief regional overview was used to build the case for Event 3 occurring most probably in the age range of 1400–1500 AD. A series of semi-continuous pebble–gravel sheets or sand and pebble units are relatively densely spread around the coastline of the northern North Island (Fig. 7). Similar groupings of pebble–gravel sheets however, can be found at other locations (e.g. W coast, North Island: Wilkes, 1995; NE coast, South Island: McFadgen and Goff, 2007) but these represent geographically distinct clusters. The maximum elevations for the sites considered here are shown in Fig. 7. There is a marked clustering to the northernmost part of the North Island, with other notably high elevations recorded on N to NW facing aspects. This presents a perplexing problem because run-up heights with coarse deposits of this nature suggest an extremely large event, but there is no obvious regional or local source (Fig. 6). Eastern sources such as the TKT and southern Kermadec volcanoes may well produce tsunamis that will refract around the northern end of the country, but wave heights decrease markedly and numerical modelling cannot replicate the magnitude of inundation (Walters et al., 2006). In a simplistic approach to try and resolve this issue we considered that the geographical spread and orientation of high elevation sites

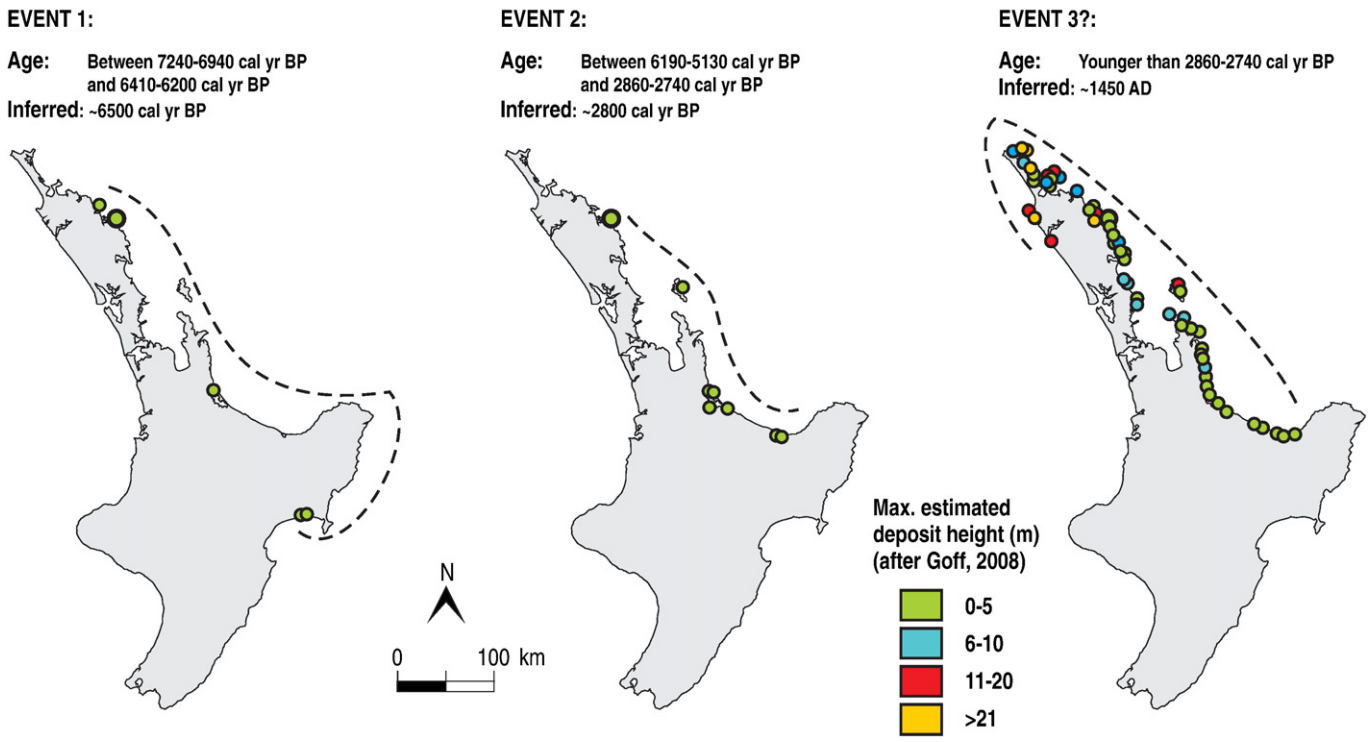


**Fig. 7.** Regional synthesis of palaeotsunami data. The Kaituna Bay, Mimiwhangata site is marked by a larger green circle (partially obscured in Event 3). The dashed line encompasses the estimated regional extent for each event.

represented wave approach from the NNW. This indicates a source from a tectonically active region that includes New Caledonia, Vanuatu and the boundary between the Fiji and Australian Plate (Fig. 1a). Palaeotsunami and palaeoseismic data for this region are extremely limited (e.g. Taylor et al., 1990; Goff et al., 2008b), but rudimentary numerical modelling of relevant subduction zone sources cannot replicate the deposit dataset (Berryman, 2005). The only other possible *known* source is the Kuwae eruption of 1452/1453 AD (K: Fig. 1a). This has been assigned a Volcanic Explosivity Index of 7, and was larger than the Tambora eruption of 1815 AD (Self, 2006). Its eruption led to the formation of a 12 km long and 6 km wide oval-shaped submarine caldera with two distinct basins and a total area of 60 $km^2$ at the level of the rim (Monzier et al., 1994). It had a minimum 100 $km^3$ of pyroclastic deposits and eruptive mass of $1\times10^{14}$ (Witter and Self, 2007; Self, 2006; Gao et al., 2006). The volcanic dust is recorded in 33 ice core records, 13 from the Northern Hemisphere and 20 from the Southern Hemisphere (Gao et al., 2006). The nature and extent of the tsunami generated by this eruption however, is largely unknown (Goff et al., 2008b). The possibility of Kuwae as a source is intriguing, but considerably more research is needed to resolve this problem. The source for Event 3 therefore remains unclear. It is worth noting however, that seafloor topographic features such as the Lord Howe Rise (LHR), Norfolk Ridge (NR), Vening Meinesz Fracture Zone (VMFZ), Three Kings Ridge (TKR), Colville Ridge (CR) and Kermadec Ridge (KR) can all act as wave guides to focus tsunamis approaching from the N on to the western, northern, or northeastern coasts of the North Island (Fig. 6).

The ability to reasonably infer potential tsunami source areas for prehistoric events has been greatly enhanced for countries such as New Zealand by the development of regional and national palaeotsunami databases. This is particularly relevant for Pacific Island Countries that have a diverse range of potential tsunami sources and source areas to choose from. The ability to determine the magnitude and frequency of events from specific source areas will improve further as national databases become more comprehensive and can be merged into regional syntheses (Goff and Dominey-Howes, 2009). This in turn will greatly enhance our understanding of the regional risk from tsunamis.

## 8. Conclusions

A multi-proxy study of contiguous wetland catchments has produced a record of environmental changes spanning the past 8000 years or more. A gradual change through the Holocene marine transgression into a modern freshwater system is punctuated by three distinct marine inundations. These have been interpreted as tsunami inundations occurring about 6500 cal yr BP, 2800 cal yr BP, and 1450 AD. By linking these with contemporaneous events in the region we have tentatively identified potential sources. On balance, the most likely source area for the two oldest events is the Tonga–Kermadec Trench region. The recent c. 1450 AD event is anomalous. The c. 1450 AD event represents a significantly higher energy inundation than the earlier events, and we have linked it regionally with a large number of similar sites in northern North Island, New Zealand. Identifying a source for this palaeotsunami however, is problematic. We have raised the possibility that it could be linked with the massive eruption of the Kuwae caldera in 1452/1453 AD.

Multi-proxy data have proven to be invaluable in determining the origins of the three overwash deposits. By considering a wider range of proxies than the more conventional suite of sediment grain size and diatoms and/or foraminifera, we have been able to draw stronger conclusions about the likely tsunamigenic nature of the deposits. Coupling these findings with a regional synthesis has further enhanced our interpretations. There is considerable value in this approach and as the databases of Australasian and Pacific palaeotsunamis grow we should be able to use this type of analysis more effectively in the future.

## Acknowledgements

This study was undertaken as a Masters Degree research thesis by SP at The University of Auckland under the supervision of SLN, JRG and

MH. Funding to support fieldwork and for radiocarbon dating was provided by Northland Regional Council. We acknowledge and thank the Department of Conservation (Whangarei) for permission to collect cores from Mimiwhangata Coastal Park.

## References


Allan, H.H., 1961. Flora of New Zealand. DSIR, Wellington.

American Society for Testing and Materials (ASTM), 1995. Standard test method for sieve analysis of fine and coarse aggregates. American Society for Testing and Materials, West Conshohockem, PA.

Ballantine, W.J., Grace, R.V., Doak, W.T., 1973. Mimiwhangata Marine Report. Turbott & Halstead and New Zealand Breweries Limited, Auckland.

Bedford, S., 2006. Pieces of the Vanuatu puzzle: archaeology of the north, south and centr. Terra Australis, 23. ANU E Press, Canberr.

Berryman, K. (compiler), 2005. Review of tsunami hazard and risk in New Zealand. MCDEM Report No. 2005/104, Ministry of Civil Defence & Emergency Management, Wellington.

Blomqvist, S., Larsson, U., 1994. Detrital bedrock elements as tracers of settling resuspended particulate matter in a coastal area of the Baltic Sea. Limnology and Oceanography 39, 880–896.

CANZ, 1997. New Zealand region bathymetry, New Zealand Oceanographic Institute Miscellaneous Chart Series 73, 3 rd ed. National Institute of Water and Atmosphere Research, Wellington.

Chagué-Goff, C., 2010. Chemical signatures of palaeotsunamis: a forgotten proxy. Marine Geology 271, 67–71.

Chagué-Goff, C., Fyfe, W.S., 1996. Geochemical and petrographical characteristics of a domed bog, Nova Scotia: a modern analogue for temperate coal deposits. Organic Geochemistry 24, 141–158.

Chagué-Goff, C., Goff, J.R., 1999. Geochemical and sedimentological signatures of catastrophic saltwater inundations (tsunami), New Zealand. Quaternary Australasia 17, 38–48.

Chagué-Goff, C., Dawson, S., Goff, J.R., Zachariasen, J., Berryman, K.R., Garnett, D.L., Waldron, H.M., Mildenhall, D.C., 2002. A tsunami (c. 6300 years BP) and other Holocene environmental changes, northern Hawke's Bay, New Zealand. Sedimentary Geology 150, 89–102.

Chagué-Goff, C., Nichol, S.L., Jenkinson, A.V., Heijnis, H., 2000. Signatures of natural catastrophic events and anthropogenic impact in an estuarine environment, New Zealand. Marine Geology 167, 285–301.

Dahanayake, K., Kulasena, N., 2008. Recognition of diagnostic criteria for recent- and paleo-tsunami sediments from Sri Lanka. Marine Geology 254, 180–186.

de Lange, W.P., Healy, T.R., 1986. New Zealand tsunamis 1840–1982. New Zealand Journal of Geology and Geophysics 29, 115–134.

Devoy, R.J., 1983. Preparation of fossil diatoms. Unpublished, Cork.

Dominey-Howes, D., 2007. Geological and historical records of tsunami in Australia. Marine Geology 239, 99–123.

Dominey-Howes, D., Humphreys, G., Hesse, P., 2006. Tsunami and palaeotsunami depositonal signatures and their potential value in understanding the late-Holocene tsunami record. The Holocene 16, 1095–1107.

Dominik, J., Stanley, D.J., 1993. Boron, berrylium and sulfur in Holocene sediments and peats of the Nile Delta, Egypt: their use as indicators of salinity and climate. Chemical Geology 104, 203–216.

Dulhunty, J.A., 1944. Origin of New South Wales torbanites. Proceedings of theLinnean Society of New South Wales 69, 26–48.

Foged, N., 1979. Diatoms in New Zealand, the North Island. Vaduz Cramer, Auckland.

Gao, C., Robock, A., Self, S., Witter, J.B., Steffenson, J.P., Clausen, H.B., Siggaard-Andersen, M.-L., Johnsen, S., Mayewski, P.A., Ammann, C., 2006. The 1452 or 1453 A.D. Kuwae eruption signal derived from multiple ice core records: Greatest volcanic sulfate event of the past 700 years. Journal of Geophysical Research 111, D12107. doi:10.1029/2005JD006710.

Gibb, J.G., 1986. A New Zealand regional Holocene eustatic sea-level curve and its application to determination of vertical tectonic movements. A contribution to IGCP-Project 200. Royal Society of New Zealand Bulletin 24, 377–395.

Goff, J.R., 2008. The New Zealand Palaeotsunami Database. NIWA Technical Report 131, ISSN 1174–2631, 24 pp + Appendix.

Goff, J.R., Chagué-Goff, C., 1999. A Late Holocene record of environmental changes from coastal wetlands: Abel Tasman National Park, New Zealand. Quaternary International 56, 39–51.

Goff, J.R., Dominey-Howes, D., 2009. Australasian palaeotsunami — do Australia and New Zealand have a shared prehistory? Earth Science Reviews 97, 147–154.

Goff, J.R., McFadgen, B.G., 2002. Seismic driving of nationwide changes in geomorphology and prehistoric settlement — a 15th Century New Zealand example. Quaternary Science Reviews 21, 2313–2320.

Goff, J.R., Chagué-Goff, C., Nichol, S.L., 2001. Palaeotsunami deposits: a New Zealand perspective. Sedimentary Geology 143, 1–6.

Goff, J., Charley, D., Haruel, C., Bonte-Grapentin, M., 2008b. Preliminary findings of the geological evidence and oral history of tsunamis in Vanuatu. SOPAC Technical Report No.416. 49 pp.

Goff, J.R., Hicks, D.M., Hurren, H., 2007. Tsunami geomorphology in New Zealand. National Institute of Water & Atmospheric Research Technical Report No. 128. 67 pp.

Goff, J.R., McFadgen, B.G., Wells, A., Hicks, M., 2008a. Seismic signals in coastal dune systems. Earth Science Reviews 89, 73–77.

Goff, J.R., Nichol, S.L., Kennedy, D., in press. Development of a palaeotsunami database for New Zealand. Natural Hazards. doi:10.1007/511069-009-9461-5.

Goff, J.R., Rouse, H.L., Jones, S.L., Hayward, B.W., Cochran, U.A., Mclea, W., Dickinson, W.W., Morley, M.S., 2000. Evidence for an earthquake and tsunami about 3100–3400 yr ago, and other catastrophic saltwater inundations recorded in a coastal lagoon, New Zealand. Marine Geology 170, 231–249.

Gorman, R.M., Bryan, K.R., Laing, A.K., 2003. Wave hindcast for the New Zealand region: nearshore validation and coastal wave climate. New Zealand Journal of Marine and Freshwater Research 37, 567–588.

Grapes, R., 2000. Magnitude Eight Plus: New Zealand's biggest earthquake. Victoria University Press, Wellington.

Hawkes, A.D., Bird, M., Cowie, S., Grundy-Warr, C., Horton, B., Tan Shau Hwai, A., Law, L., Macgregor, C., Nott, J., Eong Ong, J., Rigg, J., Robinson, R., Tan-Mullins, M., Tiong Sa, T., Zulfigar, Y., 2007. The sediments deposited by the 2004 Indian Ocean Tsunami along the Malaysia–Thailand Peninsula. Marine Geology 242, 169–190.

Hayward, B.W., Grenfell, H.R., Reid, C.M., Hayward, K.A., 1999. Recent New Zealand shallow-water benthic foraminifera: taxonomy, ecologic distribution, biogeography, and use in paleoenvironmental assessment. 258 pp.

Horrocks, M., Nichol, S.L., D'Costa, D.M., Augustinus, P., Jacobi, T., Shane, P.A., Middleton, A., 2007. A Late Quaternary record of natural change and human impact from Rangihoua Bay, Bay of Islands, northern New Zealand. Journal of Coastal Research 23, 592–604.

Horton, B.P., Hawkes, A., Engelhart, S., Bird, M., Cowie, S., Eong Ong, J., Tan Shau Hwai, A., Law, L., MacGregor, C., Tiong Sa, T., 2006. The taphonomy of sediments deposited by the Indian Ocean tsunami along the West Coast of the Malay–Thai Peninsula. AGU, pp. 43B–1237. abstract.

Hughes, J.F., Mathewes, R.W., 2003. A modern analogue for plant colonization of paleotsunami sands in Cascadia. The Holocene 13, 879–888.

Jankaew, K., Atwater, B., Sawai, Y., Choowong, M., Charoentitirat, T., Martin, M., Prendergast, A., 2008. Medieval forewarning of the 2004 Indian Ocean tsunami in Thailand. Nature 455, 1228–1231.

Jorissen, F.J., 1988. Benthic foraminifera from the Adriatic Sea: principles of phenotypic variation. Utrecht Micropalaeontological Bulletin 37 176 pp.

King, D., Goff, J.R., Skipper, A., 2007. Māori environmental knowledge and natural hazards in New Zealand. Journal of the Royal Society of New Zealand 37, 59–73.

Kortekaas, S., Dawson, A.G., 2007. Distinguishing tsunami and storm deposits: an example from Martinhal, SW Portugal. Sedimentary Geology 200, 208–221.

Krammer, K., Lange-Bertalot, H., 1997c. Bacillariophyceae: 1. Teil: Naviculaceae. In: Ettle, H., Gerloff, J., Heynig, H., Mollenhauer (Eds.), Süβwasserflora von Mitteleuropa. Spektrum Akademisher Verlag.

Krammer, K., Lange-Bertalot, H., 1997d. Bacillariophyceae: 2. Teil: Bacillariaceae, Epithemiceae, Surirellaceae. In: Ettle, H., Gerloff, J., Heynig, H., Ettle, H., Gerloff, J., Heynig, H., Mollenhauer (Eds.), Süβwasserflora von Mitteleuropa. Spektrum Akademisher Verlag.

Krammer, K., Lange-Bertalot, H., 1997a. Bacillariophyceae: 3. Teil: Centrales, Fragilariaceae, Eunotiaceae. In: Ettle, H., Gerloff, J., Heynig, H., Mollenhauer (Eds.), Süβwasserflora von Mitteleuropa. Spektrum Akademisher Verlag.

Krammer, K., Lange-Bertalot, H., 1997b. Bacillariophyceae: 4. Teil: Achnanthaceae, Kritische Ergaenzung zu Navicula (Lineolate) und Gomphonema. In: Ettle, H., Gerloff, J., Heynig, H., Mollenhauer (Eds.), Süβwasserflora von Mitteleuropa. Spektrum Akademisher Verlag.

Lamarche, G., Joanne, C., Collot, J.-Y., 2008. Successive, large mass-transport deposits in the south Kermadec fore-arc basin, New Zealand: the Matakaoa Submarine Instability Complex. Geochemistry, Geophysics, Geosystems 9, Q04001. doi:10.1029/2007GC001843.

Lloyd, E.F., Nathan, S., Smith, I.E.M., Stewart, R.B., 1996. Volcanic history of Macauley Island, Kermadec Ridge, New Zealand. New Zealand Journal of Geology and Geophysics 39, 295–308.

López-Buendia, A.M., Bastida, J., Querol, X., Whateley, M.K.G., 1999. Geochemical data as indicators of paleosalinity in coastal organic-rich sediments. Chemical Geology 157, 235–254.

Lowe, L.E., Bustin, R.M., 1985. Distribution of sulfur forms in six facies of peats in the Fraser River Delta. Canadian Journal of Soil Sciences 65, 531–541.

Macphail, M.K., McQueen, D.R., 1983. The value of New Zealand pollen and spores as indicators of Cenozoic vegetation and climates. Tuatara 26, 37–59.

Mamo, B., Strotz, L., Dominey-Howes, D., 2009. Tsunami deposits and their foraminiferal assemblages. Earth Science Reviews 96, 263–278.

McCann, W.R., Nishenko, S.P., Sykes, L.R., Krause, J., 1979. Seismic gaps and plate tectonics: seismic potential for major boundaries. Pure and Applied Geophysics 117, 1082–1147.

McCormac, F.G., Hogg, A.G., Blackwell, P.G., Buck, C.E., Higham, T.F.G., Reimer, P.J., 2004. SHCal04 Southern Hemisphere Calibration 0–11.0 cal kyr BP. Radiocarbon 46, 1087–1092.

McFadgen, B.G., 2007. Hostile shores: catastrophic events in pre-historic New Zealand and their impact on Maori coastal communities. Auckland University Press, New Zealand. 298 pp.

McFadgen, B.G., Goff, J.R., 2007. Tsunamis in the archaeological record of New Zealand. Sedimentary Geology 200, 263–274.

Monecke, K., Finger, W., Klarer, D., Kongko, W., McAdoo, B.G., Moore, A.L., Sudrajat, S.U., 2008. A 1,000-year sediment record of tsunami recurrence in northern Sumatra. Nature 455, 1232–1234.

Monzier, M., Robin, C., Eissen, J.-P., 1994. Kuwae (1425 A.D.): the forgotten caldera. Journal of Volcanology and Geothermal Research 59, 207–218.

Moore, P.D., Webb, J.A., Collinson, M.E., 1991. Pollen Analysis. Blackwell, London.

Morton, R.A., Goff, J.R., Nichol, S., 2008. Hydrodynamic implications of textural trends in sand deposits of the 2004 tsunami in Sri Lanka. Sedimentary Geology 207, 56–64.

Narayana, A.C., Tatavarti, R., Shinu, N., Subeer, A., 2007. Tsunami of December 26, 2004 on the southwest coast of India: post-tsunami geomorphic and sediment characteristics. Marine Geology 242, 155–168.
Nichol, S.L., Goff, J.R., Devoy, R.J., Chagué-Goff, C., Hayward, B., James, I., 2007a. Lagoon subsidence and tsunami on the West Coast of New Zealand. Sedimentary Geology 200, 248–262.
Nichol, S., Goff, J., Regnauld, H., 2003b. Cobbles to diatoms: facies variability in a paleo-tsunami deposit. Proceedings of the Coastal Sediments 2003 "Crossing Disciplinary Boundaries" The Fifth International Symposium on Coastal Engineering and Science of Coastal sediment processes, Florida, USA.
Nichol, S., Goff, J.R., Regnauld, H., 2004. Sedimentary evidence for a regional tsunami on the NE coast of New Zealand. Geomorphologie: Relief, Processus, Environnement 1, 35–44.
Nichol, S.L., Lian, O.B., Carter, C.H., 2003a. Sheet-gravel evidence for a late Holocene tsunami run-up on beach dunes, Great Barrier Island, New Zealand. Sedimentary Geology 155, 129–145.
Nichol, S., Lian, O.B., Horrocks, M., Goff, J.R., 2007b. Holocene Record of Gradual, Catastrophic, and Human-Influenced Sedimentation from a Backbarrier Wetland, Northern New Zealand. Journal of Coastal Research 23, 605–617.
Peters, R., Jaffe, B., Gelfenbaum, G., Peterson, C., 2003. Cascadia Tsunami Deposit Database. USGS Open-File Report 03-13.
Peters, R., Jaffe, B., Gelfenbaum, G., 2007. Distribution and sedimentary characteristics of tsunami deposits along the Cascadia margin of western North America. Sedimentary Geology 200, 372–386.
Self, S., 2006. The effects and consequences of very large explosive volcanic eruptions. Philosophical Transactions of the Royal Society A 364, 2073–2097.
Smith, D.E., Shi, S., Cullingford, R.A., Dawson, A.G., Dawson, A., Firth, C.R., Foster, I.D.L., Fretwell, P.T., Haggart, B.A., Holloway, L.K., Long, D., 2004. The Holocene Storegga Slide tsunami in the United Kingdom. Quaternary Science Reviews 23, 2291–2321.
Strotz, L., 2003. Holocene Foraminifera from Tuross Estuary and Coila Lake, south coast, New South Wales: a preliminary study. Proceedings of the Linnean Society of New South Wales 124, 163–182.
Stuiver, M., Polach, H.A., 1977. Discussion–reporting $^{14}C$ data. Radiocarbon 19, 355–363.
Switzer, A., Pucillo, K., Haredy, R.A., Jones, B.G., Bryant, E.A., 2005. Sea level, storm, or tsunami: enigmatic sand sheet deposits in a sheltered coastal embayment from southeastern New South Wales. Australia. Journal of Coastal Research 21, 655–663.
Taylor, F.W., Edwards, R.L., Wasserburg, G.J., Frohlich, C., 1990. Seismic recurrence intervals and timing of aseismic subduction inferred from emerged corals and reefs of the Central Vanuatu (New Hebrides) frontal arc. Journal of Geophysical Research 95 (B1), 393–408.
Terrell, J.E., Pope, K.O., Goff, J.R., in press. Chapter 3: Context and relevance. In: Terrell, J.E., Schechter, E.M. (Eds), Archaeological Investigations on the Sepik Coast, Papua New Guinea. Field Museum of Natural History, Chicago.
Van der Werff, A., Huls, H., 1960. Diatmeenflora van Nederland. Otto Koeltz Science Publication, Koenigstein.
Van der Werff, A., Huls, H., 1961. Diatmeenflora van Nederland. Otto Koeltz Science Publication, Koenigstein.
Van der Werff, A., Huls, H., 1962. Diatmeenflora van Nederland. Otto Koeltz Science Publication, Koenigstein.
Varekamp, J.C., 1991. Trace element geochemistry and pollution history of mudflat and marsh sediments from the Connecticut coastline. Journal of Coastal Research 11, 105–123.
Walters, R.A., Goff, J.R., Wang, K., 2006. Tsunamigenic sources in the Bay of Plenty, New Zealand. Science of Tsunami Hazards 24, 339–357.
Wilkes, O., 1995. Site recording, site types, and site distribution on the King Country coastline. Archaeology in New Zealand 38, 236–256.
Witter, J.B., Self, S., 2007. The Kuwae (Vanuatu) eruption of AD 1452: potential magnitude and volatile release. Bulletin of Volcanology 69, 301–318.
Witter, R.C., 2008. Prehistoric Cascadia tsunami inundation and runup at Cannon Beach, Clatsop County, Oregon. State of Oregon Department of Geology and Mineral Industries. Open-File Report O-08-12.
Wright, I.C., Gamble, J.A., Shane, P.A.R., 2003. Submarine silicic volcanism of the Healy caldera, southern Kermadec arc (SW Pacific): I — volcanology and eruptive mechanisms. Bulletin of Volcanology 65, 15–29.
Wright, I.C., Worthington, T.J., Gamble, J.A., 2006. New multibeam mapping and geochemistry of the 30°–35° sector, and overview of southern Kermadec volcanism. Journal of Volcanology and Geothermal Research 149, 263–296.
Yassini, I., Jones, B.G., 1989. Estuarine foraminiferal communities in Lake Illawarra, N.S.W:. Proceedings of the Linnean Society of New South Wales 110, 229–266.
Yassini, I., Jones, B.G., 1995. Foraminiferida and ostracoda from estuarine and shelf environments on the southeastern coast of Australia. University of Wollongong Press, Wollongong.